Virtual Screening against Metalloenzymes for Inhibitors and Substrates[†]

John J. Irwin,[‡] Frank M. Raushel,[§] and Brian K. Shoichet*,[‡]

*Department of Pharmaceutical Chemistry, University of California, San Francisco, 1700 4th Street,
San Francisco, California 94143-2550, and Department of Chemistry, P.O. Box 30012, Texas A&M University,
College Station, Texas 77842-3012*

ABSTRACT: Molecular docking uses the three-dimensional structure of a receptor to screen databases of small molecules for potential ligands, often based on energetic complementarity. For many docking scoring functions, which calculate nonbonded interactions, metalloenzymes are challenging because of the partial covalent nature of metal−ligand interactions. To investigate how well molecular docking can identify potential ligands of metalloenzymes using a "standard" scoring function, we have docked the MDL Drug Data Report (MDDR), a functionally annotated database of 95 000 small molecules, against the X-ray crystal structures of five metalloenzymes. These enzymes included three zinc proteases, the nickel analogue of an iron enzyme, and a molybdenum metalloenzyme. The ability of the docking program to retrospectively enrich the annotated ligands as high-scoring hits for each enzyme and to calculate proper geometries was evaluated. In all five systems, the annotated ligands within the MDDR were enriched at least 20 times over random. To test the approach prospectively, a sixth target, the zinc β-lactamase from *Bacteroides fragilis*, was screened against the fragment-like subset of the ZINC database. We purchased and tested 15 compounds from among the top 50 top-ranked ligands from docking, and found 5 inhibitors with apparent K_i values less than 120 μM, the best of which was 2 μM. A more ambitious test still was predicting actual substrates for a seventh target, a Zn-dependent phosphotriesterase from *Pseudomonas diminuta*. Screening the Available Chemicals Directory (ACD) identified 25 thiophosphate esters as potential substrates within the top 100 ranked compounds. Eight of these, all previously uncharacterized for this enzyme, were acquired and tested, and all were confirmed experimentally as substrates. These results suggest that a simple, noncovalent scoring function may be used to identify inhibitors of at least some metalloenzymes.

Metalloenzymes are important therapeutic targets, having attracted interest for diseases such as cancer (*1*, *2*), arthritis (*3*), glaucoma (*4*), and infectious disease (*5*), among others. There has been considerable interest in the structural bases for their actions, and the structures of many metalloenzyme targets have been determined. These structures have provided templates for atomic resolution modeling of reaction mechanism and for inhibitor discovery.

A problem faced in modeling metalloenzymes is the key role played by the metal. Molecular mechanics potential functions, which underlie most modeling approaches, have been parametrized to treat molecules as interacting either covalently or noncovalently. Metal−ligand interactions fit uncomfortably into either of these categories. Whereas vibrational spectroscopy indicates the presence of a metal ligand bond consistent with a force field treatment, the dative covalent "bond" is nearly an order of magnitude weaker than a covalent bond between first and second row elements. Further complicating the calculations is the unusually high charge of the metal and, to a lesser extent, the ligand, which results in high electrostatic interactions and large desolvation penalities. The free energy of binding, the difference of these two large terms, is itself relatively small, resulting in a large sensitivity to the calculation of these terms. Whereas this is a problem with nonmetal based interactions too, the magnitude of the energies involved is typically smaller. There has thus been considerable work on deriving useful parameters for metal centers in proteins.

Much effort has gone into developing force field parameters for metalloenzymes (*6*, *7*), and, at a higher level of theory, quantum mechanics based functions (*8*). More empirically, Shelver's group has optimized zinc parameters to reproduce ligand geometries from 14 crystal structures of matrix metalloproteinase having a diverse set of ligands (*9*). They report optimized zinc parameters as 0.87 Å for the radius and 0.35 kcal/mol for the well depth, which corresponds well with other reports (*7*). Confounding generality, they find that the optimal charge on zinc is +0.95 e for carboxylate inhibitors but +2.0 e for a hydroxamic acid inhibitor. Yet another empirical approach, deriving force-field parameters from experimental bond length and bond angle distributions in the Cambridge Crystallographic Database, was used to develop force-field parameters for metal−ligand interactions within four different force-field frameworks (*10*).

* Corresponding author. E-mail: shoichet@cgl.ucsf.edu. Phone: (415) 514-4126. Fax: (415) 514-4260.
[‡] University of California, San Francisco.
[§] Texas A&M University.

Notwithstanding the potential problems with the classical, parameter-based approach to treating metal centers, some progress has also been made in reproducing experimentally observed binding geometries, which is important for virtual screening. Recent reports of success at reproducing docked geometries include the targets matrix metalloproteinases (*11, 12*) and carbonic anhydrase (*13*). Molecular docking methods have also been used for lead optimization starting from a structure of the dizinc enzyme leucine aminopeptidase (*14*) and similarly for hydroxamic acid ligands against histone deacetylase (*15*). Wollmann's group used docking to predict structure—activity relationships in a series of tetrahydroiso-quinoline-3-carboxylates against MMP-8 (*16*). Several other successful computational efforts to design inhibitors of metalloenzymes have also appeared recently (*17, 18*).

These reports suggest that computational methods can reproduce geometries and, sometimes, relative binding affinities for metalloenzyme ligands. Thus, in principle, metalloenzymes are good targets for structure-based screening approaches, such as molecular docking of compound databases. However, there is reason to worry that the problems of treating the metal center, found in any molecular mechanics based approach, will become even more acute for docking screens. In docking one not only has the problem of balancing the metal—ligand interaction with the other, classical, terms in the scoring function, but one also has the problem of distinguishing likely ligands from the vast majority of the database that are "decoys". To be practical, the scoring function should be fast enough to screen hundreds of thousands of ligands in a short time, usually days, yet sensitive enough to rank previously unknown ligands high enough so that they will be recognized and tested. There are few reports of the use of virtual screening against metalloenzymes to prospectively discover novel inhibitors that are subsequently confirmed by experimental testing. The work of Pang's group on inhibitor discovery against farnesyltransferase (*19*) (but see also ref *20*) and the work of Zheng's group on peptide deformylase inhibitors (*21*) are two of the few examples available.

It seemed interesting, therefore, to explore just how far one could get with database docking screens against metalloenzymes using a classical scoring scheme—treating the metals as atoms as any others in the enzyme, with van der Waals radii and potentials, point charges, and nothing else. To do so, we retrospectively tested the ability of a docking program to screen a large compound database against disparate metalloenzymes and identify annotated ligands from among a much larger set of decoy molecules in the database. We used 95 000 compounds from the MDL Drug Data Report (MDDR),[1] which has the advantage of having functional annotations for many of its ligands. We targeted enzymes for which at least 20 ligands were annotated; each metalloenzyme typically had several ligand—enzyme complexes in the PDB. The quality of the docking screen was judged based on the enrichment of the annotated ligands among the top-scoring hits and reproduction of experimental

geometries. For any given enzyme, the annotated ligands constituted between 0.02% and 0.4% of the total database; the remaining database molecules were considered decoys.

We find docking against zinc metalloenzymes to be reliable for certain well-behaved targets, and report the results of docking screens against three of these: carbonic anhydrase II (CA II), matrix metalloproteinase-3 (MMP-3), and neutral endopeptidase (NEP). We were also able to satisfactorily dock to a nickel-containing metalloenzyme, peptide deformylase (PDF), and a molybdenum containing enzyme, xanthine oxidase (XO). Docking studies were typically less successful against heme-containing enzymes, possibly because of greater difficulties in treating iron centers through a classical scoring function, or possibly because of the much less stringent geometrical constraints imposed by heme sites compared to those of zinc and even nickel and molybdenum. We do not consider these systems further here. In an effort to test this procedure *prospectively*, we also docked 33 000 molecules from the fragment-like subset of the ZINC database (*22*) against the structure of the zinc β-lactamase from *Bacteroides fragilis*, an antibiotic resistance target for which no inhibitors are available for clinical use (*23, 24*). We experimentally tested several of these predicted, novel molecules for inhibition of the enzyme. More ambitiously still, we prospectively screened for substrates of the Zn-phosphotriesterase from *Pseudomonas diminuta*, an enzyme that hydrolyzes phosphonate esters including the nerve gas agents sarin and VX. Docking the Available Chemicals Directory (ACD, MDL, San Leandro CA), we tested eight top scoring ligands, previously unknown as substrates, that contained a hydrolyzable group consistent with the known activity of the enzyme.

MATERIALS AND METHODS

Database Preparation. The 2000.2 version of the MDDR (MDL, San Leandro, CA) was prepared as previously described (*25*). The dockable version of the ACD was prepared in a similar fashion, yielding a database of 234 000 molecular entities and about 167 000 unique compounds. Numerous functional groups including sulfonamides, thiols, and betahydroxynitrobenene moieties were prepared in both neutral and anionic form. The ZINC database was used as supplied from the Web site http://zinc.docking.org (*22*). A detailed description of protonation rules used is given in that paper (*22*).

Binding Site Preparation. Each receptor was prepared for docking in a similar manner. A grid-based excluded volume map was calculated using DISTMAP (*26*). CHEMGRID (*27*) was used to calculate an AMBER-based (*27*) van der Waals potential for the receptor. DelPhi (*28*) was used to calculate an electrostatic potential for the receptor, using an internal dielectric of 2 and an external dielectric of 78. The ligand desolvation penalty was calculated as previously described (*29*). To approximate the effect of ligand binding, the effective dielectric of the binding site was reduced by identifying the volume occupied by ligand atoms as a low dielectric region, as previously described (*30*).

Special Treatment of Metals. The following changes to our standard docking protocol were made to cope with the special characteristics of metal centers. In calculating the volume-excluded grid using DISTMAP, the metal ion was removed

---

from the model to allow ligands to approach the metal. Since DISTMAP is used to screen, not score orientations, this change has no impact on the docking scores, merely allowing more configurations to be evaluated. In calculating the van der Waals potential using CHEMGRID, ionic radii and well depths were selected for each metal. From a study of zinc binding proteins (*6*), a well depth of 0.25 kcal/mol and a radius of 1.09 Å were used to calculate parameters sqrt(A) = 53.67 and sqrt(B) = 7.33 for the Lennard-Jones calculation. In the absence of appropriate parameters for nickel and molybdenum, and considering that they were being treated as simple point charges in our model, we simply used zinc parameters for nickel and standard AMBER magnesium parameters for molybdenum. Admittedly, some of these choices were ad hoc, but pragmatically the docking calculations were not very sensitive to the exact values of the A and B Lennard-Jones terms.

We recognize that a histidine in the absence of zinc has a different charge distribution than a histidine coordinating zinc. As a rule of thumb, we chose to redistribute 0.2 electron from each coordinating group on to the metal. Thus in carbonic anhydrase II, each coordinating histidine transfers 0.2 electron from the metal-coordinating N-epsilon atom to the zinc atom, resulting in a net charge on zinc of +1.4 and a net charge on each coordinating histidine of +0.2. In bimetallic enzymes, the metals were treated independently; thus the charge on the two zincs in metallo β-lactamase and PTE was +1.4 each. This simplistic rule was applied consistently, except for xanthine oxidase. In this case, the structure report (*31*) indicates some ambiguity about the precise chemical identity of atoms coordinating molybdenum. We have assumed a formal oxidation state of VI on Mo, and have assumed that the ligands quench all but +1.0 of the positive charge on Mo. The iron sulfide cluster, and the ligands of Mo, were treated as occupying space but were silent in the electrostatic map.

Ligand atoms from the crystal structure augmented with selected SPHGEN spheres served as matching positions (spheres) to orient database molecules in the site. These positions defined the orientations sampled by the ligand in the site, using the DOCK matching algorithm in which sets of receptor site positions are matched against sets of ligand atom positions (*32*).

Molecular Docking. We used DOCK3.5.54 to flexibly dock the ligands into the active site of each receptor, based on a hierarchical method of sampling ligand conformations (*26*, *33*). To sample ligand orientations (see Supporting Information, Table S1), bin sizes varied for each system. Over all systems, ligand and receptor bins were set to 0.3−0.5 Å and overlap bins were set to 0.2−0.4 Å; the distance tolerance for matching ligand atoms to receptor matching sites was in the range 1.2−1.5 Å. Each ligand configuration was sampled for steric fit; those passing the steric filter were scored for combined electrostatic and van der Waals complementarity. Each energy score was adjusted by an electrostatic and an apolar desolvation term calculated for each ligand by the program AMSOL (*34*), as described (*35*). This desolvation cost was adjusted based on the orientation adopted by the ligand in the binding site according to how buried any given ligand atom was by the receptor (our unpublished method). The best-scoring conformation for any given ligand orientation was then minimized with 100 steps

of simplex rigid-body minimization (*36*). Docking calculations took about a few days to a week CPU time per enzyme on a Linux 2.4 GHz Xeon system (Table S1). Between 3500 and 10 000 orientations per molecule were sampled, and at each orientation, thousands of conformations were sampled, depending on the molecule's conformational flexibility.

Ligand Identification. All molecules annotated in the MDDR as an inhibitor target were initially counted as ligands for the appropriate metalloenzyme. For CA II, only ligands annotated "carbonic anhydrase" were used. For PDF, no MDDR annotated molecules were available, so we augmented our database of annotated ligands by preparing a database from literature studies (see below) using ISIS/Draw (MDL, San Leandro CA), WebLab (Accelrys, San Diego, CA), and thereafter our usual protocol using the Filter and Omega programs (OpenEye Software, Santa Fe NM), AMSOL (*34*), and mol2db (part of the DOCK suite).

For each docking calculation, all molecules in the MDDR that could be fit in the site were ranked by their energy score. For molecules represented in multiple protonation or other states in the database, only the top-scoring form of each molecule was kept. This rank-ordered list was then divided into 1000 bins (of 96 molecules each). The ability of DOCK to identify annotated ligands from all the docked MDDR molecules was evaluated based on the cumulative percentage of known molecules found in each bin and the enrichment factor over random selection, calculated as described (*35*).

Materials. Zinc β-lactamase from *B. fragilis* was a gift of Prof. Marvin Mackinen of the University of Chicago. ZINC database compounds 403452, 338282, 284503, 35810, 105246, 403452, 99997 were purchased from Sigma Aldrich (St. Louis, MO); ZINC database compounds 336937 and 334995, 335033, 335250, 245638, 53704 were purchased from Specs (Delft, The Netherlands); 156339 was purchased from Ryan Scientific (Isle of Palms, SC). For phosphotriesterase, ACD compounds 55449 (fenthion), 36204 (diazinon), 55407 (fenitrothion) were purchased from ChemService (West Chester, PA). All other compounds tested against phosphotriesterase were ordered from Sigma-Aldrich. Nitrocefin was purchased from Oxoid Ltd (Basingstoke, England), and HEPES was purchased from Sigma-Aldrich (St. Louis, MO). All materials were used as supplied by the manufacturer, without future purification.

Enzyme Assays. Compounds were tested for inhibition of zinc β-lactamase using nitrocefin as a substrate. Unless otherwise stated, assays were performed in 50 mM HEPES buffer, pH 7.3 at 24.0 °C. Stocks of nitrocefin and inhibitors were generally prepared in dimethyl sulfoxide (DMSO), except for thiol-containing compounds, which were prepared in aqueous buffer. No more than 5% DMSO was present in any assay, and results were controlled for the presence of DMSO. All reactions were monitored on a HP8453 spectrophotometer. The K_m of nitrocefin was 5.8 μM under these conditions. All assays were initiated by addition of enzyme and run in the presence of 0.01% Triton X-100 to prevent aggregation-based inhibition (*37*). Only inhibitors that were insensitive to detergent are reported here. In our experience, aggregation-based, promiscuous inhibition is common among virtual and high throughput screening hits and must be controlled for. Phosphotriesterase assays were performed as previously described (*38*).

Table 1: Enzymes Targeted for Retrospective Docking

enzyme name	PDB code	metal	resolution (Å)	no. of known inhibitors[a]
CA II	1cil	Zn	1.6	241
MMP-3	1hy7	Zn	1.5	337
NEP	1dmt	Zn	2.1	184
PDF	1lqy	Ni	1.9	21[a]
XO	1fiq	Mo	2.5	74

[a] Inhibitors annotated in the MDDR database except for PDF which were added to the MDDR from the literature (*64*).

Table 2: Retrospective Docking Results against Five Metalloenzymes

enzyme name	max enrichment factor	% of database to find 25% of ligands	% of database where max enrichment occurred
CA II	82	1.6	0.1
MMP-3	32	3.2	0.1
NEP	189	0.2	0.1
PDF	47	0.7	0.8
XO	36	1.0	0.6

RESULTS

Overview. We begin with a dramatic approximation: that for docking purposes we can treat catalytic metal centers in enzymes as classical interaction centers, defined by van der Waals radii and well depths, and by point charges. This classical approximation was tested in retrospective calculations against five metalloenzymes (Table 1). Performance was measured by reproducing experimental geometries and by the enrichment of known inhibitors from among a large majority of decoy molecules in large database screens. Two more enzymes were targeted for prospective docking for inhibitors (for a metallo-β-lactamase) and substrates (for a zinc phosphotriesterase), where we were looking for genuinely new ligands. These were tested experimentally.

To parametrize the metal ions, we drew on earlier work in the field, assigning to zinc ions a van der Waals radius of 1.09 Å and a well-depth minimum of 0.25 kcal/mol, in broad agreement with literature values (*6*). These parameters were used for each zinc enzyme we targeted. For the nickel enzyme peptide deformylase, we also used a van der Waals radius of 1.09 Å and a well depth of 0.25 kcal/mol. For the molybdenum enzyme xanthine oxidase, we used a van der Waals radius of 1.17 Å and a well depth of 0.1 kcal/mol for molybdenum.

One area where we diverged somewhat from literature procedures was in the assignment of formal charges to the metal. Because of the close involvement of ligating residues on the protein, and the expectation of charge-transfer events between the metals and these protein groups, we transferred some of the metal ion net charge from the metal center to the ligating protein residues. Starting from the AMBER charge model and a +2 formal charge on zinc, a net charge of +0.2 was transferred from the zinc to each of the ligating residues, leaving a net charge of +1.4 on each zinc and a net charge of +0.2 on each histidine or other ligating residue. For dizinc enzymes, each metal was treated independently, with no charge transfer taking place between the zincs. This admittedly ad hoc charge redistribution scheme turned out to be broadly in line with model calculations at the Hartree−Fock and MP2 levels (Supporting Information, Table S2). Since there are several uncertainties in a quantum mechanical calculation, such as truncation effects from using a restricted number of residues for the model, and since the simple charge redistribution scheme seems to work satisfactorily, we have used it throughout this work.

Docking calculations were judged to be successful only if the structure of representative ligand-bound structures from the PDB could be reproduced within 2 Å rmsd of the crystallographic coordinates and a satisfactory enrichment above random could be achieved. Enrichment was evaluated using four criteria: the maximum "enrichment factor" (*39*) of the annotated ligands among the ranked hits, the percentage of the docking-ranked MDDR database necessary to look through to find 25% of the annotated ligands, overall profiles of enrichment factors and percentage of ligands found as a function of the ranked database (Table 2 and Figure 1), and the geometry of the docked ligands compared to that observed crystallographically (Figure 2). The "enrichment factor" is defined as the number of annotated ligands found, at any given point in the dock-ranked list of compounds, divided by the number of ligands one would expect to find at random. For instance, if a system had 95 annotated ligands in a database of 95 000 molecules, one would expect to find 1 ligand per bin of 1000 database molecules by random selection alone. If a docking screen ranked 10 ligands in the top-scoring 1000 molecules, this would represent a 10-fold improvement over random selection (a 10-fold enrichment factor) for this bin.

In subsequent sections we consider the performance of each individual system in detail. We then turn to consider prospective predictions versus the zinc β-lactamase from *B. fragilis* (CcrA) and phosphotriesterase from *P. diminuta*.

Carbonic Anhydrase II (CA II). Carbonic anhydrase II inhibitors are used in the treatment of glaucoma to lower the intraocular pressure, which reduces aqueous humor production (*40*). This has been an active area of research, with 11 drugs developed, and consequently there are 241 CA II inhibitors in the MDDR. A 1.6 Å ligand-bound structure of human form of CA II from the PDB (code 1cil (*41*)) was used for docking. The zinc ion is coordinated by three histidines, with N−Zn distances in the range of 2.0− 2.1 Å. Most of the annotated inhibitors of CA II are arylsulfonamidates, in which the N and often one of the O atoms of the sulfonamidate group coordinate the metal. The aryl group of the ligand occupies a narrow hydrophobic pocket composed of Val121, Leu198, and Thr200 (Figure 2A).

We began by redocking the crystallographic inhibitor, ETS. The molecule was prepared using our standard protocol, including precalculating partial atomic charges using AMSOL (*34*) (*35*) and multiple ligand conformations using Omega (OpenEye Software). The high-scoring docked geometry was 0.4 Å rms from the crystal structure (Figure 2Ai); the lowest rms pose was 0.3 Å from the crystallographic geometry and was the second ranked in energy. Docking the MDDR, we looked at how well the known inhibitors were enriched as top hits relative to the rest of the database molecules, which we considered decoys. The highest enrichment factor was reached among the top-scoring 0.1% of the ranked database and was 82-fold over random (Table 2, Figure 1A); it was possible to dock 229 of the
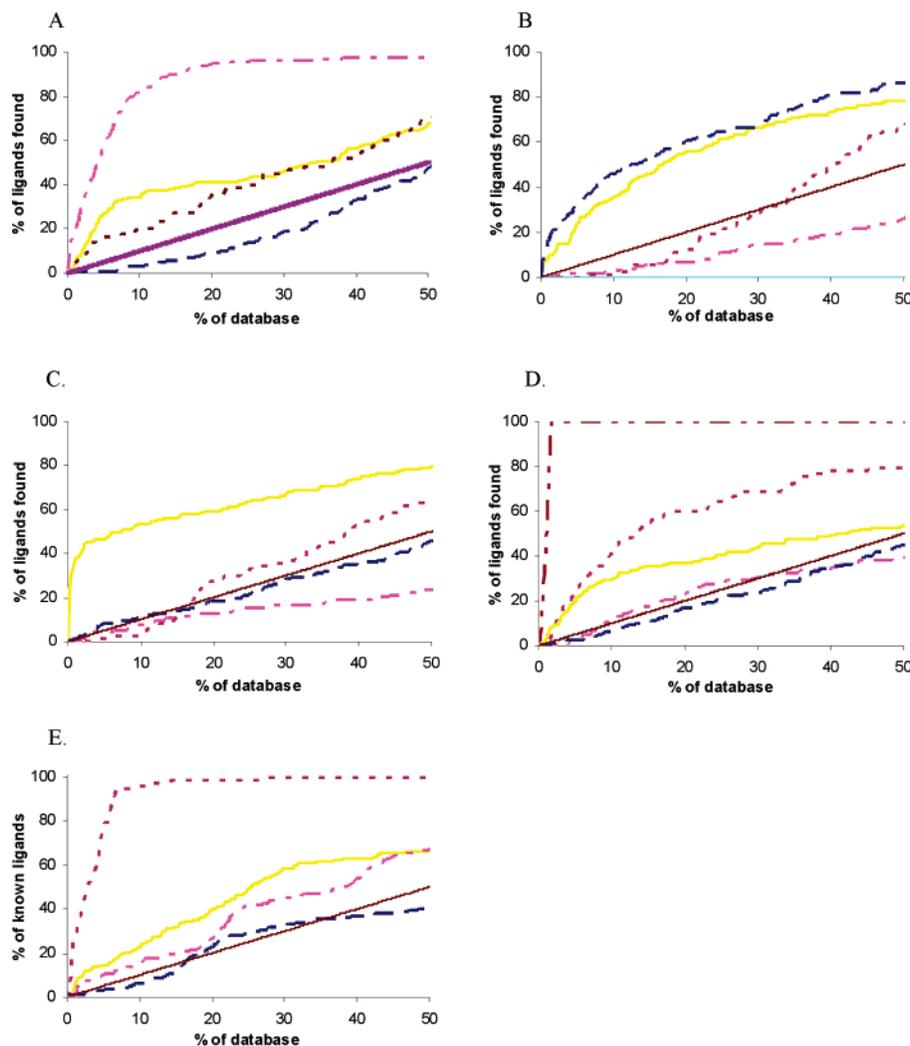
FIGURE 1: Enrichment plots of the five ligand classes against each of five metalloenzymes: (A) carbonic anhydrase II; (B) matrix metalloproteinase-3; (C) neutral endopeptidase; (D) peptide deformylase; (E) xanthine oxidase. The symbols for the ligand classes are as follows: for the 241 carbonic anydrase ligands, − - −; for the 337 matrix metalloproteinase ligands, − −; for the 184 neutral endopeptidases, −; for the 21 peptide deformylase ligands, − - -; for the 74 xanthine oxidase ligands, - - - -. Random enrichment is indicated by a thin black diagonal line. Each panel shows the cumulative percentage of annotated ligands found vs the percentage of the docking rank-ordered database. For each target, the enrichments of ligands from the other four targets are shown in addition to that of the cognate ligands.

annotated ligands into the receptor, 25% of which were identified in the top 1.6% of the database, docked in poses that resembled that of the crystallographic ligand (Figure 2Aii).

To capture the anionic nature of the arylsulfonamidates, which is induced on binding, all sulfonamides in the database were represented in both ionized and neutral forms; both states were represented when docking against all of the metalloenzymes. The negatively charged, deprotonated sulfonamidates scored much better than the neutral form, although both were docked in poses resembling those observed crystallographically. Intriguingly, many of the high scoring "decoys" for this site were labeled as antiglaucoma agents. We suspect that these are also CA II inhibitors, but treated them as decoys to be conservative.

Matrix Metalloproteinase-3 (MMP-3). Human fibroblast stromelysin (also called matrix metalloproteinase-3) is a proteoglycanase with a wide range of substrates. Matrix metalloproteinases have attracted interest as therapeutic targets for arthritis (*42*), neuronal injury (*43*), osteoporosis (*44*), and rheumatoid arthritis (*45*), and there are 337

inhibitors annotated as MMP inhibitors in the MDDR. There is little distinction in the MDDR among inhibitors acting on the different subclasses of MMP enzymes. We have thus treated all of the annotated MMP inhibitors in the MDDR as though they were MMP-3 inhibitors. This was largely done as a matter of convenience, but it is not unreasonable for our purposes since the different MMPs share a highly conserved active site. A 1.5 Å ligand-bound structure of the enzyme (PDB code 1hy7 (*46*)) was used for docking. Again, the zinc ion is coordinated by three histidine side chains, with N−Zn distances falling in the range 2.1−2.2 Å. The known MMP inhibitors in the MDDR are chemically diverse, but are dominated by molecules that coordinate the zinc via hydroxamate, carboxylate, thiol, or sulfonamidate moieties. Most ligands occupy the deep, narrow hydrophobic P1 binding pocket, formed by the residues Val698, Tyr723, His701, and Leu718. The rest of the binding site is quite open, as expected for a protease.

We begin by docking the crystallographic inhibitor, MBS. The high-scoring docked geometry was 0.7 Å rms from the crystal structure (Figure 2Bi); the lowest rms pose was 0.4
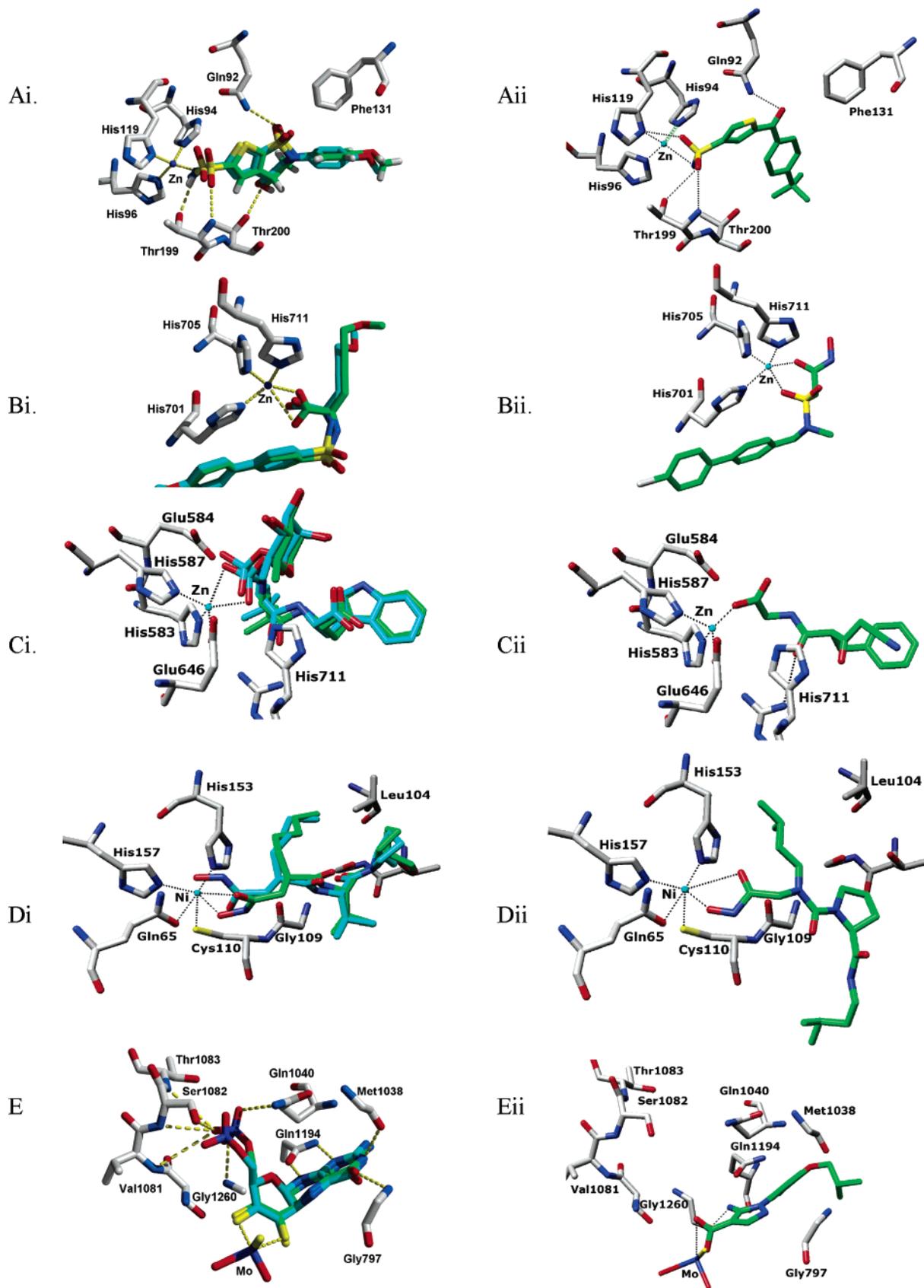
FIGURE 2: Molecular docking poses: (A) carbonic anhydrase II; (B) matrix metalloproteinase-3; (C) neutral endopeptidase; (D) docked peptide deformylase; (E) xanthine oxidase. (i) In each panel, the crystallographic ligand is depicted with carbon atoms in cyan, the docking ligand with carbon atoms in green. Hydrogen bonds and metal−ligand interactions between the docked ligand and the enzyme are shown with dashed lines. (ii) The docked geometry of a top scoring ligand directly from the MDDR database screening calculation: (Aii) CA II. MDDR210444 (rank 6). (Bii) MMP-3. MDDR280126 (rank 14). (Cii) NEP. MDDR172890 (rank 13). (Dii) Peptide deformylase. Compound ID 4390 (rank 102). (Eii) Xanthine oxidase. MDDR266275 (rank 262).

Å from the crystallographic geometry and was the sixth ranked in energy. A total of 324 of the ligands were docked, yielding a maximum enrichment of 32-fold over random in the top 0.1% of the database (Figure 1B, Table 2). Docking found 25% of the known inhibitors in the top 3.2% of the database (Figure 2Bii).

Neutral Endopeptidase (NEP). Neutral endopeptidase is involved in the degradation of atrial natriuric factor (ANF) and is implicated in heart failure; the enzyme has thus been a therapeutic target (*47*). The 184 annotated NEP inhibitors in the MDDR are structurally diverse, sharing little other than a central peptide bond, a metal coordinating moiety, and a large hydrophobic group, such as a biphenyl. The phosphoramidon-bound human enzyme, determined to 2.1 Å, was used for docking (PDB code 1dmt (*48*)). The zinc ion is coordinated by two histidines with Zn−N distances of 2.0 Å and a glutamate having a Zn−O distance also of 2.0 Å. The binding site is a narrow groove, with a neighboring small hydrophobic pocket formed by Ile558, Val580, Trp693, and Phe106 (Figure 2C).

We began by redocking the crystallographic inhibitor, RDF. The high-scoring docked geometry was 1.2 Å rms from the crystal structure (Figure 2Ci); the lowest rms pose was 0.9 Å from the crystallographic geometry and was the 9th ranked in energy. Docking the MDDR yielded a maximum enrichment of 189-fold over random in the top 0.1% of the database (Figure 1C, Table 2). The top 25% of ligands were found in the top 0.2% of the database. The geometry of a typical ligand docked into the binding site and superimposed on its crystal structure pose is shown (Figure 2Cii). Ligands that scored well but were not annotated as inhibitors were as diverse as the annotated ligands themselves, but normally had at least one large hydrophobic moiety and a charged group such as a carboxylate or phosphate, as did the annotated ligands.

Peptide Deformylase (PDF). Peptide deformylase is an essential metalloenzyme required for the removal of the formyl group at the N terminus of nascent polypeptide chains in eubacteria. The *Escherichia coli* enzyme uses Fe^{2+} and retains its activity (*49*) on substitution of the metal ion by Ni^{2+}. Although peptide deformylase inhibitors are not annotated in the MDDR, five ligand-bound crystal structures with Fe^{2+} or Ni^{2+} are available from the PDB (*50−52*) and 21 inhibitors have recently been described (*53*), which were added to our database for docking. A 1.9 Å Ni-containing structure was used for docking (PDB code 1lqy (*49*)). The nickel is coordinated by His153, His157, Gln65, and Cys110 (Figure 2D). The crystallographic ligand, actinonin, a naturally occurring antibacterial agent, coordinates the nickel via both oxygens of the hydroxamate group (Figure 2Di).

We began by redocking the crystallographic inhibitor, actinonin. The high-scoring docked geometry was 0.9 Å rms from the crystal structure; the lowest rms pose was 0.7 Å from the crystallographic geometry and was the 5th ranked in energy. Docking the MDDR led to a maximum of 47-fold enrichment over random in the top 0.8% of the database (Table 2, Figure 1D). Twenty-five percent of the ligands were found in the top 0.7% of the database; the docked geometries were reasonable (Figure 2Dii).

Xanthine Oxidase (XO). Xanthine oxidase produces oxidative free radicals, and inhibitors of this enzyme have been used to study endothelial dysfunction in cigarette smokers

Table 3: New Inhibitors of Metallo *β*-Lactamase from *B. fragilis*

ZINC Code	Molecular Structure	Rank (out of 33,000)	Apparent K_i (µM)
336937		1	130
338282		2	14
35810		18	90
99997		24	3
403452		33	2
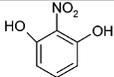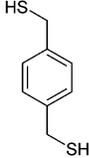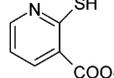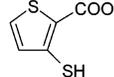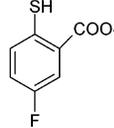
(*54*). The 2.5 Å mammalian ligand-bound structure was used for docking (PDB code 1fiq (*31*)). We docked to the Mo−pterin binding site with the pterin removed, since the annotated ligands in the MDDR are pterin analogues. The coordination around Mo is octahedral, with three atoms holding down adjacent positions, and the remaining face of the Mo atom is free to coordinate with ligands. In the crystal structure, the pterin coordinates the Mo using two exocyclic thiocarbonyls.

We began by redocking the crystallographic pterin cofactor, MTE. The high-scoring docked geometry was 0.7 Å rms from the crystal structure; the lowest rms pose was 0.5 Å from the crystallographic geometry and was the 2nd ranked in energy. A total of 74 inhibitors in the MDDR were available, of which 73 could be docked. Maximum enrichment achieved was 36-fold over random in the top 0.6% of the database (Table 2, Figure 1E). Twenty-five percent of ligands were found in the top 1.0% of the database. The docked geometries of the inhibitors were reasonable (Figure 2Eii).

Thus the enrichment factors in the retrospective tests were relatively high. To control for the possibility that this enrichment owed simply to size selection, we compared the molecular weight distribution of the annotated ligands for each target against that of the entire MDDR database. The distribution of molecular weights in each ligand class overlap that of the MDDR well (Supporting Information, Figure S1). A further control is to compare the enrichment factors of ligands for *other* metalloenzymes to that of the cognate ligands for any given target. In each case, the enrichment factor for the cognate ligands was significantly higher than that of the metalloenzyme ligands from other classes (Figure 1). These controls suggest that the high enrichment factors do not simply reflect a size bias nor selection for metal-chelating groups alone.
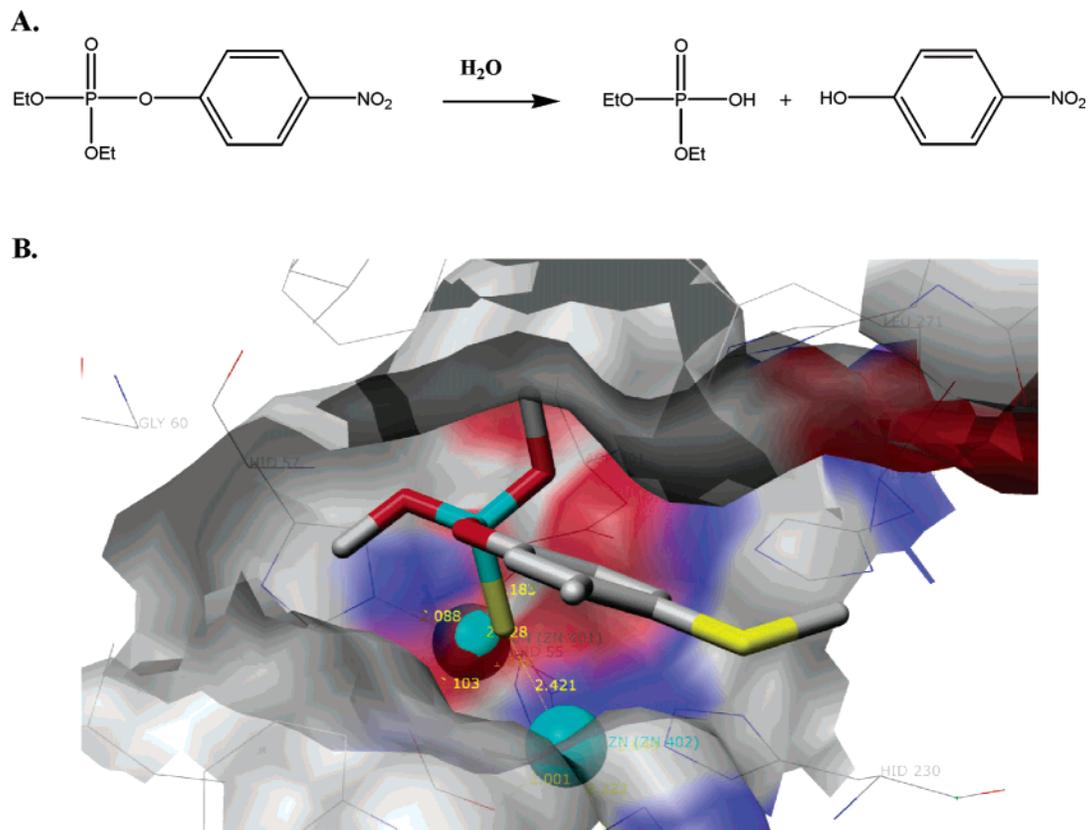
FIGURE 3: Bacterial phosphotriesterase: (A) reaction mechanism; (B) docked pose of fenthion (DOCK rank 1), an experimentally confirmed substrate. Zinc ions are depicted as cyan spheres.

Zinc β-Lactamase from B. fragilis (CcrA). CcrA is a class B, zinc metallo-β-lactamase (*55*). The enzyme is a target for reversing bacterial resistance to carbapenems. X-ray crystal structures of the enzyme reveal two zinc atoms in the active site. We used the 1.85 Å PDB structure 1a7t for docking. We used the ligands from the two available complexes (PDB codes 1a7t (*56*) and 1a8t (*57*)) as controls. The biphenyl tetrazole ranked 1650 out of 167 000 ACD molecules and docked within 1.3 Å rms of the crystallographic pose. The tricyclic carboxylate inhibitor ranked 2000 in the ACD screen, and its top scoring pose was 1.1 Å rms from the crystallographic pose. Whereas these rankings are less than ideal, the docking screen nevertheless captured the key ligand binding interactions and reproduced the experimental geometries.

For prediction of novel inhibitors, we then docked the "fragment-like" subset of the ZINC database (*22*), which became available while this project was underway. "Fragment-like" is defined here as having a molecular weight of 250 or less, a calculated log P between -2 and 3, fewer than three hydrogen-bond donors and six hydrogen-bond acceptors, and fewer than three rotatable bonds. Fragment-based screening is currently popular for novel ligand discovery, as it affords new scaffolds with options for follow on synthetic elaboration (*58*). In control calculations, we found that a number of annotated ligands had high-ranking docking scores. For example, 2-sulfanylbenzoic acid (ZINC284503) which is reported as a broad spectrum metallo β-lactamase inhibitor (*59*), ranked 13th in our ZINC database screen. The 18th ranked 2-sulfanylnicotinic acid (ZINC35810) and the 33rd ranked 5-fluoro-2-sulfanylbenzoic

acid (ZINC403352) are similar to ZINC284503, and both were confirmed experimentally as inhibitors with apparent K_i values of 90 μM and 2 μM, respectively. A further reported inhibitor, dipicolinic acid (ZINC105246) (*60*), ranked 30th. We purchased 15 compounds from among the top 50 docking hits for experimental testing. Of these, five showed significant inhibition below 120 μM (Table 3), the best having an apparent K_i of 2 μM.

All of the docking hits put one electronegative group (usually the thiolate) in the μ^2-bridging position between the two zincs, the location of the hydroxide nucleophile during catalysis (Figure 4). The other electronegative group interacted with Lys164. There were a dozen compounds in the top 100 that resembled the five novel inhibitors that we did find; we suspect that these may also inhibit the enzyme, but they were not tested.

We wanted to control for the possibility that any small molecule with approximately the right sort of "hot" functionality such as hydroxamate, carboxylate, or thiolate would inhibit CcrA. To do so, we purchased and tested benzyl-hydroxamic acid and observed no inhibition at 200 μM. We also tested 10 low molecular weight thiols available in the lab from other projects, only one of them showing slight inhibition at 200 μM. These results suggest that the docking calculations are capturing more than simple presence of a hot, metal-binding functionality such as thiols and hydroxamates.

Phosphotriesterase from P. diminuta (PTE). PTE is a dizinc metalloenzyme that hydrolyzes the phosphorus—oxygen bond of phophodiesters and phosphotriesters, including organophosphorus nerve agents including the insecticide

i.

ii.

iii.
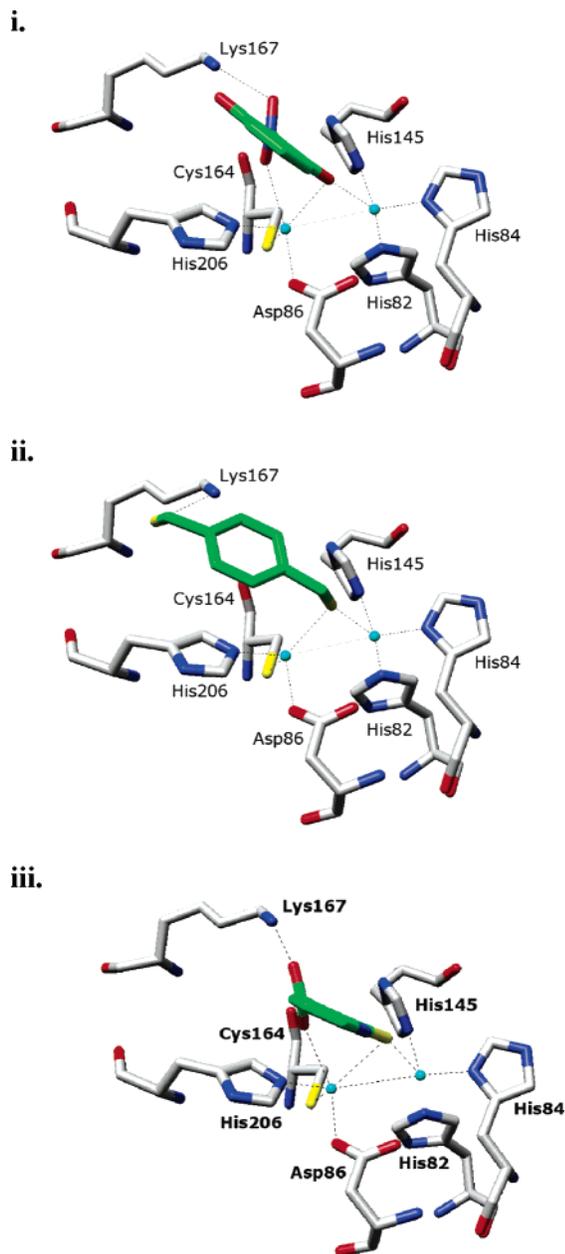
FIGURE 4: Docked geometries of top scoring hits against the metallo-β-lactamase from *B. fragilis*. Metal atoms are cyan spheres. Distances from ligand to zinc atoms and Lys NZ shown.

paraoxon and the chemical warfare agents sarin, soman, and VX (*38*, *61*) (Figure 3A). We used a 1.8 Å crystal structure (1hzy from the PDB (*62*)). Zn β is coordinated by His230, His201, the side chain O of carboxylated Lys169, and Zn β. Zn α is coordinated by His55, His57, Asp301, and the O of carboxylated Lys169. The hydroxide nucleophile is stabilized by the two zincs and Asp301.

In an attempt to discover novel substrates of phosphotriesterase, we docked 167 000 commercially available compounds of the 2001.1 version of the ACD (MDL, San Leandro CA) into a structure of the apo-enzyme with the hydroxide removed. Methyl parathion, a well-known substrate and thus a control for our calculations, ranked 8th out of 167 000. A number of similar compounds not known to be substrates also ranked very highly. A representative example is parathion ethyl, which ranked 28th, and docked

such that the S atom of the thiophosphate ester occupied the μ^2 bridging position between the two zincs, a position normally occupied by the hydroxide nucleophile during catalysis (Figure 3B). The rest of this potential substrate made no specific polar interaction in the binding site, but was held in place by van der Waals interactions. Parathion ethyl and seven other related molecules, all previously unknown as substrates for phosphotriesterase, were tested experimentally in an enzyme assay; all were found to be, in fact, substrates for the enzyme, with K_{cat}/K_m values ranging from 2.5×10^3 to 10^6 s^{-1} M^{-1} (Table 4).

DISCUSSION

Metalloenzymes are challenging targets for virtual screening because of the covalent-like interaction between the metal centers and their ligands and the large electrostatic potentials of the metals. Here, we took a simple approach to these enzymes, using a standard noncovalent scoring function with molecular mechanics parameters for the metals. Four noteworthy results emerge from this study. First, for most enzymes, docking achieved relatively high enrichment factors in database screens, performing no less well than one would expect for nonmetal enzyme targets. Second, there were several targets for which the simplification of ignoring the covalent nature of the metal failed—these were often heme-iron sites where the approximations are farther from reality than for full-shell metals such as zinc. Third, new inhibitors of CcrA zinc β-lactamase were predicted and experimentally tested. Fourth, and perhaps most surprisingly, new substrates were predicted for the zinc phosphotriesterase from *P. diminuta*.

The geometric fidelity and enrichment factors emerging from docking to the five zinc, nickel, and molybdenum enzymes was as successful as we might expect to see for well-behaved nonmetal targets (Table 2). Enrichment factors were high, ranging from 32 to 189 in large database screens, and the geometries of the docked ligands closely resembled the crystallographic structures. Indeed, and somewhat to our surprise, the presence of the metal often simplified matters for the docking calculation, providing a hot target for atoms bearing the correct, complementary functionality. Of course, this did require parametrization of the metals, but we found that accepted literature values for van der Waals radii and well depths were satisfactory for database screens. The largest methodological innovation we adopted was in the treatment of the charge at the metal center, which we partially distributed over the residues that ligated the metal in the absence of the inhibitor. In all systems, we treated the metal centers consistently.

Not all metalloenzymes performed well. Docking against heme-iron bearing targets, such as cytochrome P450s and nitric oxide synthases, led to generally poor docked geometries and enrichment factors little better than random (not shown). In both of these systems, ligand—metal coordination appears to be driven by electronic factors on the open face of an iron-coordinated heme group. By contrast, all the successful systems we targeted were relatively constrained around the metal. In our hands, sites where metal coordination is under steric control were appropriate for docking screens, whereas sites where metal coordination is directed by molecular orbital considerations are too difficult, at least

Table 4: Kinetic Data against Phosphotriesterase[a]

compound	Structure	dock rank (out of 167,000)	Kcat (1/s)	Km(mM)	kcat/Km (1/s M)
quinalphos		5	N.D.[*]	N.D.[*]	1.0×10^6
parathion methyl		8	105	1.0	1.0×10^5
diazinon		12	190	1.5	1.3×10^6
pirimiphos methyl		16	1.9	0.2	9.1×10^3
parathion ethyl		28	380	0.3	1.3×10^6
chorpyrifos methyl		31	0.3	0.1	2.5×10^3
chlorpyrifos		32	1.3	0.03	4.5×10^4
propetamphos		100	3.8	0.2	1.7×10^4
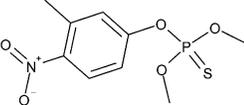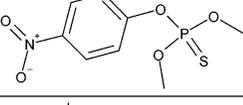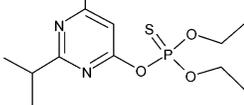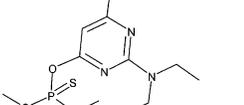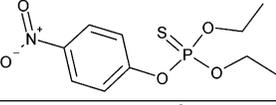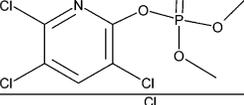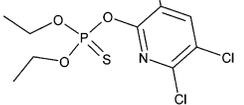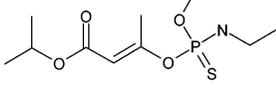
[a] ND: not determined. (*) Quinalphos did not saturate at 0.1 mM.

for our current docking algorithm. More generally, we make no claim for having "solved" the problem of predicting ligand binding energies for metalloenzymes, nor do we mean to suggest that the ad hoc treatment we employ here can be used in other applications, for instance lead optimization. Rather, we believe that for a subset of metalloenzymes where the metal center is relatively constrained sterically, using noncovalent parametrization within a classic docking scoring function is pragmatic for docking database screens.

To test the approach more convincingly, we turned to prospective prediction of inhibitors of zinc class B β-lactamase, CcrA. We docked 33 000 ligands of the "fragment-like" subset of the September 2004 version of the ZINC database (which stands for "ZINC is not commercial", and has nothing to do with metals or metalloenzymes in particular, but is meant to be a general source library for virtual screening) (*22*) (http://zinc.docking.org). Fifteen compounds from the top 50 ranked molecules from this docking screen were tested experimentally, and five were found to inhibit CcrA with apparent K_i values of 2 to 120 μM. Given that all of these inhibitors were "fragment-like", which is to say, quite small compared to drug-like molecules,

their affinities were relatively high, as were their "ligand efficiencies" (*63*). Some of the hits from this calculation were expected, such as ZINC403452 (Table 3), which closely resembles literature controls. Others, especially the top-ranked ZINC336937, were novel. Also, many functional groups known to bind to other zinc centers did not inhibit CcrA. Thus, for instance, benzohydroxamic acid and 6-sulfanylpicolinic acid, which sport a hydroxamate and a thiol, repectively, will inhibit nonspecific metal-binding centers, but they do not appear to inhibit CcrA detectibly at concentrations up to 100 μM. This suggests that the docking calculation, in addition to finding functional groups to ligate the zinc center, was also considering steric and electrostatic complementarity of the enzyme site overall. Unusually for inhibitors found through docking screens, which are often picked based on several criteria including visual inspection, here we tested exclusively molecules that were at the very top of the hit list, including those ranked 1st, 2nd, 4th, 13th 18th, 24th, 30th, and 33rd. Five of these turned out to be micromolar inhibitors of the enzyme.

As in most virtual screens, treatment of the molecules in the database was an important factor in docking against

CcrA, and indeed all the metalloenzymes discussed here. For instance, the top scoring hit, 2-nitrobenzene-1,3-diol, a 130 μM inhibitor of CcrA on testing, was docked in the neutral, monohydroxide anion and dihydroxide anion forms, as indicated by heuristic deprotonation rules. The dianionic form scored best. Deprotonation of hydroxide groups ortho to nitro groups on an aromatic ring is a new feature of the ZINC database, using modified protonation/deprotonation rules implemented in the program ligprep (Schrodinger Inc). Without correctly deprotonating the diol of the nitrobenzene, this compound would not have scored in the top 500. The first pK_a of this compound is 4.7, and the second is 7.0, so it is quite appropriate that the dianionic form should have scored well. Correct deprotonation was important for a number of other top hits. Thus, the second ranked hit, [2-(sulfanylmethyl)phenyl]methanethiol, a 14 μM inhibitor on testing, was docked as a dithiolate anion. The other experimentally confirmed hits in Table 3 all owe their top ranking to correctly deprotonating the thiolate.

Perhaps the most surprising and compelling result to emerge from this study was the prediction and experimental testing of new substrates for the enzyme PTE. We make no general claim to being able to distinguish substrates from inhibitors; typically, we are doing well if we can find ligands of any sort. We realized, however, that the docking hits for this target might just as well act as substrates as inhibitors, since they so closely resembled the known substrates. To investigate this, we considered the 100 top-scoring docking hits as possible substrates. After eliminating those without an appropriate hydrolyzable group, eight were acquired for experimental testing and all were hydrolyzed by PTE (Table 4).

Taken together, these studies suggest that structure-based virtual screening may be undertaken against at least some metalloenzymes, i.e., those where the ligand site on the metal is at least partially under steric control. For such targets, the retrospective docking screens exhibit enrichment factors no worse and often better than strictly noncovalent targets, using a classical treatment of the metal center. This is borne out by the strong results of the prospective docking screens for new inhibitors of CcrA. The prediction of substrates has few precedents in the docking literature and we cannot infer too much from this single result, except to note that it was probably made easier by the "hot" nature of the Zn center in the docking potential function. This may be a general advantage for docking to metalloenzymes.

ACKNOWLEDGMENT

SUPPORTING INFORMATION AVAILABLE

Table S1, docking statistics, including time taken and number of poses sampled for each run. Table S2, a comparison of charge models for phosphotriesterase (1hzy) using four different methods; a PDB format file of the model used in the demonstration calculation and a Jaguar input file are also included. Figure S1, molecular weight distribution of annotated ligand lists compared with the MDDR as a whole. This material is available free of charge via the Internet at http://pubs.acs.org.

REFERENCES

1. Bradshaw, R. A., and Yi, E. (2002) Methionine aminopeptidases and angiogenesis, *Essays Biochem. 38*, 65−78.
2. Kruger, E. A., and Figg, W. D. (2000) TNP-470: an angiogenesis inhibitor in clinical development for cancer, *Expert Opin. Invest. Drugs 9*, 1383−96.
3. Beaudeux, J. L., Giral, P., Bruckert, E., Foglietti, M. J., and Chapman, M. J. (2004) Matrix metalloproteinases, inflammation and atherosclerosis: therapeutic perspectives, *Clin. Chem. Lab. Med. 42*, 121−31.
4. Cvetkovic, R. S., and Perry, C. M. (2003) Brinzolamide: a review of its use in the management of primary open-angle glaucoma and ocular hypertension, *Drugs Aging 20*, 919−47.
5. Eswaramoorthy, S., Kumaran, D., and Swaminathan, S. (2002) A novel mechanism for Clostridium botulinum neurotoxin inhibition, *Biochemistry 41*, 9795−802.
6. Stote, R. H., and Karplus, M. (1995) Zinc binding in proteins and solution: a simple but accurate nonbonded representation, *Proteins 23*, 12−31.
7. Merz, K., Anderson, K., and Hoops, S. (1991) Force field design for metalloproteins, *J. Am. Chem. Soc. 113*, 8262−70.
8. Raha, K., and Merz, K. M., Jr. (2004) A quantum mechanics-based scoring function: study of zinc ion-mediated ligand binding, *J. Am. Chem. Soc. 126*, 1020−1.
9. Hu, X., and Shelver, W. H. (2003) Docking studies of matrix metalloproteinase inhibitors: zinc parameter optimization to improve the binding free energy prediction, *J. Mol. Graph Model 22*, 115−26.
10. David, L., Amara, P., Field, M. J., and Major, F. (2002) Parametrization of a force field for metals complexed to bio-macromolecules: applications to Fe(II), Cu(II) and Pb(II), *J. Comput.-Aided Mol. Des. 16*, 635−51.
11. Hu, X., Balaz, S., and Shelver, W. H. (2004) A practical approach to docking of zinc metalloproteinase inhibitors, *J. Mol. Graphics Modell. 22*, 293−307.
12. Ha, S., Andreani, R., Robbins, A., and Muegge, I. (2000) Evaluation of docking/scoring approaches: a comparative study based on MMP3 inhibitors, *J. Comput.-Aided Mol. Des. 14*, 435−48.
13. Esposito, E. X., Baran, K., Kelly, K., and Madura, J. D. (2000) Docking of sulfonamides to carbonic anhydrase II and IV, *J. Mol. Graphics Modell. 18*, 283−9, 307−8.
14. Grembecka, J., Mucha, A., Cierpicki, T., and Kafarski, P. (2003) The most potent organophosphorus inhibitors of leucine amino-peptidase. Structure-based design, chemistry, and activity, *J. Med. Chem. 46*, 2641−55.
15. Ragno, R., Mai, A., Massa, S., Cerbara, I., Valente, S., Bottoni, P., Scatena, R., Jesacher, F., Loidl, P., and Brosch, G. (2004) 3-(4-Aroyl-1-methyl-1H-pyrrol-2-yl)-N-hydroxy-2-propenamides as a new class of synthetic histone deacetylase inhibitors. 3. Discovery of novel lead compounds through structure-based drug design and docking studies, *J. Med. Chem. 47*, 1351−9.
16. Matter, H., Schudok, M., Schwab, W., Thorwart, W., Barbier, D., Billen, G., Haase, B., Neises, B., Weithmann, K., and Wollmann, T. (2002) Tetrahydroisoquinoline-3-carboxylate based matrix-metalloproteinase inhibitors: design, synthesis and structure−activity relationship, *Bioorg. Med. Chem. 10*, 3529−44.
17. Puerta, D. T., Schames, J. R., Henchman, R. H., McCammon, J. A., and Cohen, S. M. (2003) From model complexes to metallo-protein inhibition: a synergistic approach to structure-based drug discovery, *Angew. Chem., Int. Ed. 42*, 3772−4.

18. Cama, E., Shin, H., and Christianson, D. W. (2003) Design of amino acid sulfonamides as transition-state analogue inhibitors of arginase, *J. Am. Chem. Soc. 125*, 13052−7.

19. Perola, E., Xu, K., Kollmeyer, T. M., Kaufmann, S. H., Prendergast, F. G., and Pang, Y. P. (2000) Successful virtual screening of a chemical database for farnesyltransferase inhibitor leads, *J. Med. Chem. 43*, 401−8.

20. McGovern, S. L., Caselli, E., Grigorieff, N., and Shoichet, B. K. (2002) A common mechanism underlying promiscuous inhibitors from virtual and high-throughput screening, *J. Med. Chem. 45*, 1712−22.

21. Howard, M. H., Cenizal, T., Gutteridge, S., Hanna, W. S., Tao, Y., Totrov, M., Wittenbach, V. A., and Zheng, Y. J. (2004) A novel class of inhibitors of peptide deformylase discovered through high-throughput screening and virtual ligand screening, *J. Med. Chem. 47*, 6669−72.

22. Irwin, J. J., and Shoichet, B. K. (2005) ZINC—a free database of commercially available compounds for virtual screening, *J. Chem. Inf. Model. 45*, 177−82.

23. Cornaglia, G., Riccio, M. L., Mazzariol, A., Lauretti, L., Fontana, R., and Rossolini, G. M. (1999) Appearance of IMP-1 metallo-beta-lactamase in Europe, *Lancet 353*, 899−900.

24. Livermore, D. M., and Woodford, N. (2000) Carbapenemases: a problem in waiting?, *Curr. Opin. Microbiol. 3*, 489−95.

25. McGovern, S. L., and Shoichet, B. K. (2003) Information decay in molecular docking screens against holo, apo, and modeled conformations of enzymes, *J. Med. Chem. 46*, 2895−907.

26. Shoichet, B., Bodian, D. L., and Kuntz, I. D. (1992) Molecular Docking Using Shape Descriptors, *J. Comput. Chem. 13*, 380−97.

27. Meng, E. C., Shoichet, B., and Kuntz, I. D. (1992) Automated Docking with Grid-Based Energy Evaluation, *J. Comput. Chem. 13*, 505−24.

28. Gilson, M. K., and Honig, B. H. (1987) Calculation of electrostatic potentials in an enzyme active site, *Nature 330*, 84−6.

29. Wei, B. Q., Weaver, L. H., Ferrari, A. M., Matthews, B. W., and Shoichet, B. K. (2004) Testing a flexible-receptor docking algorithm in a model binding site, *J. Mol. Biol. 337*, 1161−82.

30. Lorber, D. M., and Shoichet, B. K. (1998) Flexible ligand docking using conformational ensembles, *Protein Sci. 7*, 938−50.

31. Enroth, C., Eger, B. T., Okamoto, K., Nishino, T., and Pai, E. F. (2000) Crystal structures of bovine milk xanthine dehydrogenase and xanthine oxidase: structure-based mechanism of conversion, *Proc. Natl. Acad. Sci. U.S.A. 97*, 10723−8.

32. Kuntz, I. D., Blaney, J. M., Oatley, S. J., Langridge, R., and Ferrin, T. E. (1982) A Geometric Approach to Macromolecule-Ligand Interactions, *J. Mol. Biol. 161*, 269−88.

33. Lorber, D. M., Udo, M. K., and Shoichet, B. K. (2002) Protein-protein docking with multiple residue conformations and residue substitutions, *Protein Sci. 11*, 1393−408.

34. Li, J. B., Zhu, T. H., Cramer, C. J., and Truhlar, D. G. (1998) New class IV charge model for extracting accurate partial charges from wave functions, *J. Phys. Chem. A 102*, 1820−31.

35. Wei, B. Q., Baase, W. A., Weaver, L. H., Matthews, B. W., and Shoichet, B. K. (2002) A model binding site for testing scoring functions in molecular docking, *J. Mol. Biol. 322*, 339−55.

36. Gschwend, D. A., and Kuntz, I. D. (1996) Orientational sampling and rigid-body minimization in molecular docking revisited: on-the-fly optimization and degeneracy removal, *J. Comput.-Aided Mol. Des. 10*, 123−32.

37. McGovern, S. L., Helfand, B. T., Feng, B., and Shoichet, B. K. (2003) A specific mechanism of nonspecific inhibition, *J. Med. Chem. 46*, 4265−72.

38. Dumas, D. P., Caldwell, S. R., Wild, J. R., and Raushel, F. M. (1989) Purification and properties of the phosphotriesterase from Pseudomonas diminuta, *J. Biol. Chem. 264*, 19659−65.

39. Stahl, M. (2000) Modifications of the scoring function in FlexX for virtual screening applications, *Perspect. Drug Discov. Des. 20*, 83−98.

40. Medeiros, F. A., and Weinreb, R. N. (2002) Medical backgrounders: glaucoma, *Drugs Today 38*, 563−70.

41. Smith, G. M., Alexander, R. S., Christianson, D. W., McKeever, B. M., Ponticello, G. S., Springer, J. P., Randall, W. C., Baldwin, J. J., and Habecker, C. N. (1994) Positions of His-64 and a bound water in human carbonic anhydrase II upon binding three structurally related inhibitors, *Protein Sci. 3*, 118−25.

42. Janusz, M. J., Bendele, A. M., Brown, K. K., Taiwo, Y. O., Hsieh, L., and Heitmeyer, S. A. (2002) Induction of osteoarthritis in the rat by surgical tear of the meniscus: Inhibition of joint damage by a matrix metalloproteinase inhibitor, *Osteoarthritis Cartilage 10*, 785−91.

43. Wallace, J. A., Alexander, S., Estrada, E. Y., Hines, C., Cunningham, L. A., and Rosenberg, G. A. (2002) Tissue inhibitor of metalloproteinase-3 is associated with neuronal death in reperfusion injury, *J. Cereb. Blood Flow Metab. 22*, 1303−10.

44. Martignetti, J. A., Aqeel, A. A., Sewairi, W. A., Boumah, C. E., Kambouris, M., Mayouf, S. A., Sheth, K. V., Eid, W. A., Dowling, O., Harris, J., Glucksman, M. J., Bahabri, S., Meyer, B. F., and Desnick, R. J. (2001) Mutation of the matrix metalloproteinase 2 gene (MMP2) causes a multicentric osteolysis and arthritis syndrome, *Nat. Genet. 28*, 261−5.

45. Beehler, B. C., Hei, Y. J., Chen, S., Lupisella, J. A., Ostrowski, J., Starrett, J. E., Tortolani, D., Tramposch, K. M., and Reczek, P. R. (2003) Inhibition of disease progression by a novel retinoid antagonist in animal models of arthritis, *J. Rheumatol. 30*, 355−63.

46. Natchus, M. G., Bookland, R. G., Laufersweiler, M. J., Pikul, S., Almstead, N. G., De, B., Janusz, M. J., Hsieh, L. C., Gu, F., Pokross, M. E., Patel, V. S., Garver, S. M., Peng, S. X., Branch, T. M., King, S. L., Baker, T. R., Foltz, D. J., and Mieling, G. E. (2001) Development of new carboxylic acid-based MMP inhibitors derived from functionalized propargylglycines, *J. Med. Chem. 44*, 1060−71.

47. Mulder, P., and Thuillez, C. (2002) Emerging concepts of neurohumoral modulation in the treatment of congestive heart failure, *Arch. Mal. Coeur Vaiss. 95*, 821−6.

48. Oefner, C., D'Arcy, A., Hennig, M., Winkler, F. K., and Dale, G. E. (2000) Structure of human neutral endopeptidase (Neprilysin) complexed with phosphoramidon, *J. Mol. Biol. 296*, 341−9.

49. Becker, A., Schlichting, I., Kabsch, W., Schultz, S., and Wagner, A. F. (1998) Structure of peptide deformylase and identification of the substrate binding site, *J. Biol. Chem. 273*, 11413−6.

50. Guilloteau, J. P., Mathieu, M., Giglione, C., Blanc, V., Dupuy, A., Chevrier, M., Gil, P., Famechon, A., Meinnel, T., and Mikol, V. (2002) The crystal structures of four peptide deformylases bound to the antibiotic actinonin reveal two distinct types: a platform for the structure-based design of antibacterial agents, *J. Mol. Biol. 320*, 951−62.

51. Clements, J. M., Beckett, R. P., Brown, A., Catlin, G., Lobell, M., Palan, S., Thomas, W., Whittaker, M., Wood, S., Salama, S., Baker, P. J., Rodgers, H. F., Barynin, V., Rice, D. W., and Hunter, M. G. (2001) Antibiotic activity and characterization of BB-3497, a novel peptide deformylase inhibitor, *Antimicrob. Agents Chemother. 45*, 563−70.

52. Hao, B., Gong, W., Rajagopalan, P. T., Zhou, Y., Pei, D., and Chan, M. K. (1999) Structural basis for the design of antibiotics targeting peptide deformylase, *Biochemistry 38*, 4712−9.

53. Hackbarth, C. J., Chen, D. Z., Lewis, J. G., Clark, K., Mangold, J. B., Cramer, J. A., Margolis, P. S., Wang, W., Koehn, J., Wu, C., Lopez, S., Withers, G., 3rd, Gu, H., Dunn, E., Kulathila, R., Pan, S. H., Porter, W. L., Jacobs, J., Trias, J., Patel, D. V., Weidmann, B., White, R. J., and Yuan, Z. (2002) N-alkyl urea hydroxamic acids as a new class of peptide deformylase inhibitors with antibacterial activity, *Antimicrob. Agents Chemother. 46*, 2752−64.

54. Guthikonda, S., Sinkey, C., Barenz, T., and Haynes, W. G. (2003) Xanthine oxidase inhibition reverses endothelial dysfunction in heavy smokers, *Circulation 107*, 416−21.

55. Ambler, R. P. (1980) The structure of beta-lactamases, *Philos. Trans. R. Soc. London, Ser. B 289*, 321−31.

56. Fitzgerald, P. M., Wu, J. K., and Toney, J. H. (1998) Unanticipated inhibition of the metallo-beta-lactamase from Bacteroides fragilis by 4-morpholineethanesulfonic acid (MES): a crystallographic study at 1.85-Å resolution, *Biochemistry 37*, 6791−800.

57. Toney, J. H., Fitzgerald, P. M., Grover-Sharma, N., Olson, S. H., May, W. J., Sundelof, J. G., Vanderwall, D. E., Cleary, K. A., Grant, S. K., Wu, J. K., Kozarich, J. W., Pompliano, D. L., and Hammond, G. G. (1998) Antibiotic sensitization using biphenyl tetrazoles as potent inhibitors of Bacteroides fragilis metallo-beta-lactamase, *Chem. Biol. 5*, 185−96.

58. Hartshorn, M. J., Murray, C. W., Cleasby, A., Frederickson, M., Tickle, I. J., and Jhoti, H. (2005) Fragment-based lead discovery using X-ray crystallography, *J. Med. Chem. 48*, 403−13.

59. Mollard, C., Moali, C., Papamicael, C., Damblon, C., Vessilier, S., Amicosante, G., Schofield, C. J., Galleni, M., Frere, J. M.,

and Roberts, G. C. (2001) Thiomandelic acid, a broad spectrum inhibitor of zinc beta-lactamases: kinetic and spectroscopic studies, *J. Biol. Chem. 276*, 45015−23.

60. Payne, D. J., Bateson, J. H., Gasson, B. C., Proctor, D., Khushi, T., Farmer, T. H., Tolson, D. A., Bell, D., Skett, P. W., Marshall, A. C., Reid, R., Ghosez, L., Combret, Y., and Marchand-Brynaert, J. (1997) Inhibition of metallo-beta-lactamases by a series of mercaptoacetic acid thiol ester derivatives, *Antimicrob. Agents Chemother. 41*, 135−40.

61. Donarski, W. J., Dumas, D. P., Heitmeyer, D. P., Lewis, V. E., and Raushel, F. M. (1989) Structure−activity relationships in the hydrolysis of substrates by the phosphotriesterase from Pseudomonas diminuta, *Biochemistry 28*, 4650−5.

62. Benning, M. M., Shim, H., Raushel, F. M., and Holden, H. M. (2001) High-resolution X-ray structures of different metal-substituted forms of phosphotriesterase from Pseudomonas diminuta, *Biochemistry 40*, 2712−22.

63. Abad-Zapatero, C., and Metz, J. T. (2005) Ligand efficiency indices as guideposts for drug discovery, *Drug Discovery Today 10*, 464−9.

64. Cali, P., Naerum, L., Mukhija, S., and Hjelmencrantz, A. (2004) Isoxazole-3-hydroxamic acid derivatives as peptide deformylase inhibitors and potential antibacterial agents, *Bioorg. Med. Chem. Lett. 14*, 5997−6000.